RESEARCH ARTICLE

Porphyromonas gingivalis outer membrane vesicles alter cortical neurons and Tau phosphorylation in the embryonic mouse brain

Adrienne J. Bradley[1][⚬], Lauren Mashburn-Warren[1][⚬], Lexie C. Blalock[1][⚬][¤],
Francesca Scarpetti[1], Christian L. Lauber[1,2]*

1 Institute for Genomic Medicine, Nationwide Children's Hospital, Columbus, Ohio, United States of America, 2 Department of Pediatrics, The Ohio State University College of Medicine, Columbus, Ohio, United States of America

⚬ These authors contributed equally to this work.
¤ Current Address: Abbott Nutrition, Columbus, Ohio, United States of America
* Christian.Lauber@nationwidechildrens.org
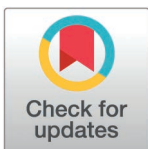
Abstract

Porphyromonas gingivalis (Pg) is an oral bacterial pathogen that has been associated with systemic inflammation and adverse pregnancy outcomes such as low birth weight and pre-term birth. Pg drives these sequelae through virulence factors decorating the outer membrane that are present on non-replicative outer membrane vesicles (OMV) that are suspected to be transmitted systemically. Given that Pg abundance can increase during pregnancy, it is not well known whether Pg-OMV can have deleterious effects on the brain of the developing fetus. We tested this possibility by treating pregnant C57/Bl6 mice with PBS (control) and OMV from ATCC 33277 by tail vein injection every other day from gestational age 3 to 17. At gestational age 18.5, we measured dam and pup weights and collected pup brains to quantify changes in inflammation, cortical neuron density, and Tau phosphorylated at Thr231. Dam and pup weights were not altered by Pg-OMV exposure, but pup brain weight was significantly decreased in the Pg-OMV treatment group. We found a significant increase of Iba-1, indicative of microglia activation, although the overall levels of IL-1β, IL-6, TNFα, IL-4, IL-10, and TGFβ mRNA transcripts were not different between the treatment groups. Differences in IL-1β, IL-6, and TNFα concentrations by ELISA showed IL-6 was significantly lower in Pg-OMV brains. Cortical neuron density was modified by treatment with Pg-OMV as immunofluorescence showed significant decreases in Cux1 and SatB2. Overall p-Tau Thr231 was increased in the brains of pups whose mothers were exposed to Pg-OMV. Together these results demonstrate that Pg-OMV can significantly modify the embryonic brain and suggests that Pg may impact offspring development via multiple mechanisms.

Introduction

Pregnancy induces significant changes in mothers including shifts in the abundance of oral bacteria [1–4]. Increased blood flow and pregnancy related hormones allows for the growth of pathogens like *Porphyromonas gingivalis* (Pg) an organism associated with oral infections that are increasingly linked to adverse pregnancy and neurodevelopmental outcomes [5–7]. Increased Pg presence is estimated to be prevalent in 40% of pregnancies in the US and 2–11% worldwide [8,9]. This presence of bacteria sometimes resulting in periodontitis, a significant dental infection, can drive systemic inflammation [10–12]. Preterm birth, preeclampsia, and low birth weight are well-characterized effects of maternal Pg infections and Pg DNA has been detected in the placenta and amnionic fluid. Pg driven outcomes affecting children have focused on pregnancy outcomes [13–18] and only recently has Pg received attention as a modulator of fetal development and remains an understudied host-pathogen interaction [19,20].

P. gingivalis has been extensively studied to determine its role in modifying pregnancy. Rodent models of Pg infection demonstrate that exposure to Pg can result in systemic inflammation, low birth weight and pre-term delivery [21–25]. Pg mediates these and other effects thorough a number of virulence factors that modify host responses including lipopolysaccharide (LPS) and proteases known as gingipains [26–32]. Both are also present on the surface of OMV that are now suspected to be transmitted systemically in the blood stream [20,32,33]. LPS and the gingipains interact with the immune system but are unique compared to other gram-negative bacteria. For instance, Pg LPS is less immunogenic than *Escherichia coli* LPS but also causes inflammation and the production of pro-inflammatory cytokines [34,35]. The gingipains are unique to Pg and they modify cytokine expression that allows Pg to evade the host immune response and establish periodontal infections that drive systemic inflammation [36–39]. Pg infection also modifies the placenta to cause spiral artery remodeling that can result in a hypoxic state linked to preeclampsia and fetal growth restriction [40]. However, whether Pg-OMV may induce fetal growth restriction—a common outcome in animal models and humans with Pg infections of clinical significance—is not yet known.

P. gingivalis is associated with maternal inflammation and adverse pregnancy outcomes that increase the risk of modified developmental trajectories of offspring [17,41]. Maternal infection and the resulting inflammation affect development though mechanisms not fully described at this time [42]. Live Pg is well demonstrated to increase inflammation in animal models and exposure to Pg-OMV recapitulates these observations as the vesicles harbor the same virulence factors. Ishida et al. reported increased Iba-1 indicative of microglia activation that was accompanied by increased inflammation and cytokine production and modified neurons in E 20 pup brains from dams with an established Pg infection prior to pregnancy [19]. Offspring from Pg infected dams also demonstrated declines in cognitive ability, and it was suggested the combined effects on the embryonic brain resulted in neuroinflammation that drove these changes. Similarly, Gong et al. described a neuroinflammatory phenotype in adult mice where exposure to Pg-OMV for 3 months increased IL-1β and NLRP3 expression concurrent with modification of the cortical neurons and behavior [33]. Together these studies suggest that long-term exposure to Pg and Pg-OMV can result in immune phenotypes indicative of a pro-inflammatory response that would be expected from activated microglia in the M1 activation state [43,44]. However, the maternal immune system functions differently than the non-pregnant state and changes in inflammation and the abundance of cortical neurons related to pathogen exposure *in utero* after pregnancy is established may also differ. This knowledge gap limits our efforts to refine predictions of the potential impact of pathogen-driven inflammation on the developmental trajectory of offspring.

Tau is an essential protein with multiple roles in maintaining neuron homeostasis [45–47]. Proper function is dependent on phosphorylation that can occur at multiple sites and can be modified by inflammation and exposure to pathogens such as Pg [48–50]. Phosphorylated Tau (p-Tau) has less affinity for tubulins and self-aggregates into β-amyloid plaques that are a hallmark of neuroinflammatory diseases such as Alzheimer's and Parkinson's diseases in older adults [51]. The resulting Tau tangles can trigger an immune response that is sustained through microglial NFκβ signaling and thus are considered pathogenic forms of the protein [52,53]. In a mouse model, Gong et al. showed that Pg-OMV alter the Tau profile and could result in β-amyloid plaques accompanied by increased inflammation [33]. However, relatively less is known about the role of p-Tau in the developing brain and whether exposure to pathogens during pregnancy alters this profile. A survey of fetal and adult Tau phosphorylation in humans demonstrated significant overlap in p-Tau where some of the pathogenic forms of Tau in adults with Alzheimer's disease were also prevalent in the fetal brain suggesting p-Tau in children does not have a pathogenic effect as observed in adults [54]. Interestingly, Tau is hyperphosphorylated in the embryonic rodent brain but knock-down of Tau during gestation in mice can reduce neuronal migration to all cortical layers indicating that p-Tau is an important part of normal brain development in mice [48,50,55]. Whether or not Pg-OMV may modulate Tau phosphorylation in developing brains *in utero* is an open question. Addressing this knowledge gap may provide valuable insight into the mechanisms by which Pg is able to modify developmental trajectories of children.

Herein, we describe a study to determine whether maternal exposure to Pg-OMV could effect the developing mouse brain to understand this host-pathogen interaction that frequently occurs in the human population. To simulate a maternal infection with Pg, pregnant C57/Bl6 mice were exposed to a consistent dose of Pg-OMV via tail vein injection. At gestational age (GA) 18.5, we measured microglia activation, pro- and anti-inflammatory cytokines, total Tau and p-Tau Thr231, and the abundance of cortical neuron proteins in embryonic pup brains. We hypothesize that maternal exposure to Pg-OMV will garner an inflammatory response where Iba-1 expression is accompanied by increased production of pro-inflammatory cytokines that have been observed in humans and animal models attempting to define the impact of Pg infections on the adult and developing brain. Moreover, we expect that Pg-OMV will change the Tau profile and modify expression of cortical neuron proteins concordat with other observations that may be relevant in defining the impact of pathogen exposure on development during pregnancy.

Results

OMV isolation and characterization

OMV from *P. gingivalis* strain ATCC 33277 were collected from cleared supernatants by ultracentrifugation and stored at − 20 C in PBS. The OMV prep contained spherical particles (S1 1A Fig) that retained gingipain activity and were comprised of LPS at 0.5 EU/ml +/- 0.09 EU (S1 1B and 1C Fig). Plots of activities and concentrations can be found in the supporting information S1.

Pup body and brain weights

Previous studies in mice have demonstrated that dams with Pg infection or those consistently dosed with Pg bacteria during pregnancy can result in low birth weight of pups. We recorded weight of the dams, pups, and pup brains at GA 18.5 (Fig 1A) to determine whether exposure to Pg-OMV would have the same effect. Dam and pup weights were not significantly different in PBS and Pg-OMV groups (Fig 1A and 1B) but there was a significant decrease in the
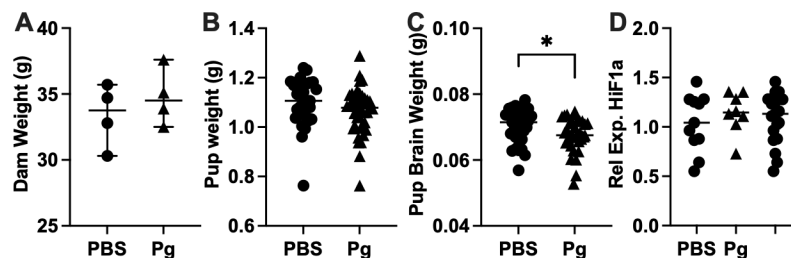
Fig 1. Dam and pup body and brain weights. (A) and **(B)** Weight of dams and pups were not significantly different from PBS controls. **(C)** Pup brain weight decreased significantly with Pg exposure (Mann-Whitney U p = 0.023). **(D)** Relative expression of Hif1a as indicator of hypoxia in the pup brain. Relative expression calculated by the $2^{-(\Delta\Delta Ct)}$ method with GAPDH as the reference gene. Data are shown as median with 95% CI.

https://doi.org/10.1371/journal.pone.0310482.g001

pup brain weight after 14 days of Pg-OMV treatment (Fig 1C, Mann-Whitney U p = 0.023). We included an assessment of Hif1a as Pg is known to cause hypoxia in mouse models that is related to fetal growth restriction. Relative expression of HiF1a in the embryonic mouse brain was not significantly different between the control and treated groups indicating the OMV did not induce a hypoxic state *in utero* that could account for the decreased pup brain weights (Fig 1D).

Inflammation

Maternal inflammation can affect the developing embryo in mouse models, and we tested whether exposure to Pg-OMV during pregnancy would result in an inflammatory response concordant with increased presence of pathogens experienced during pregnancy. In a similar approach used by Ishida et al [19], we assessed the concentration of Iba-1 as a marker of microglia activation indicative of maternal Pg infection that can lead to increased cytokine production, inflammation, and damage to neurons and may be activated by maternal factors [42,56]. Western blotting of whole brain homogenates showed that Iba-1 was significantly increased in Pg-OMV pup brains compared to PBS controls (Fig 2A and 2B, Mann-Whitney U p = 0.0003). Next, we tested whether increased Iba-1 was accompanied by increased concentration and expression of pro-inflammatory cytokines IL-1β, IL-6 and TNFα (Fig 3) indicative of M1 activation that produces a pro-inflammatory response. ELISA quantification showed that PBS pups typically had higher levels of cytokines but only IL-6 was significantly greater in the PBS brains compared to pups from the Pg-OMV group (Fig 3D, Student's T-test p = 0.002). The levels of IL-1β and TNFα showed similar trends but were not
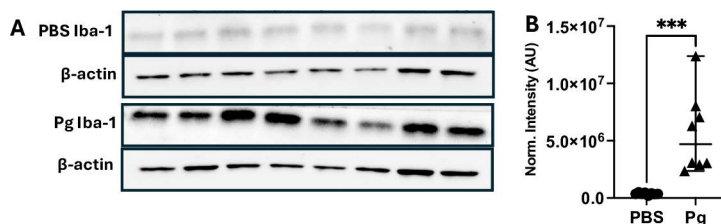
Fig 2. Increased Iba-1 in mouse pups exposed to Pg-OMV during pregnancy. (A) Western blot of Iba-1 and β-actin in GA 18.5 pups from PBS and Pg-OMV exposed dams. Full blot can be found in the Supporting information. **(B)** Comparison of β-actin normalized signal intensity of Iba-1 showed significant increase in Iba-1 in the Pg-OMV group compared to controls (Mann-Whitney U p = 0.0003). Data are shown as median with 95% CI.

https://doi.org/10.1371/journal.pone.0310482.g002
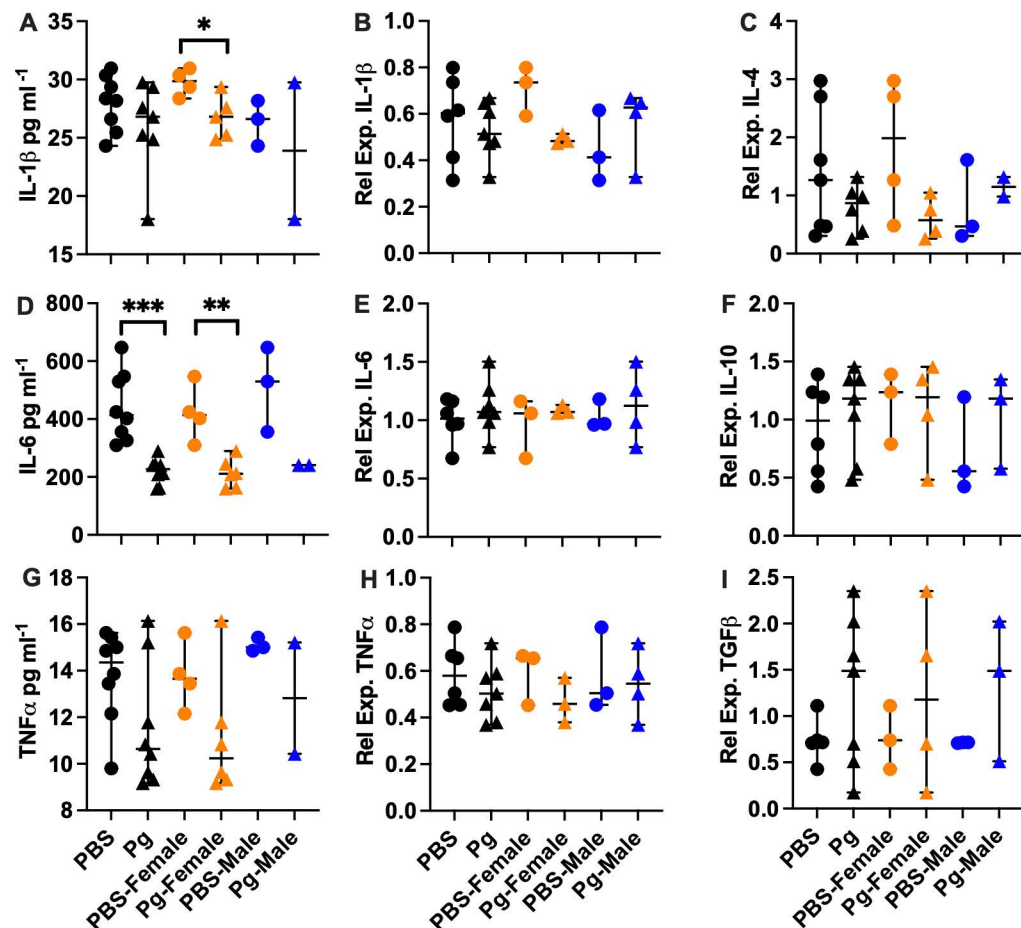
Fig 3. ELISA and RT-qPCR evaluation of cytokines in the embryonic mouse brain. (A, D, G): ELISA of IL-1β, IL-6, and TNFα in pg ml^{-1}. Cytokines were extracted from frozen whole brains and quantified. IL-1β was significantly greater in the PBS female pups compared to the female pups from the Pg-OMV group (Fig 3A, Mann-Whitney U test p = 0.04). IL-6 was significantly greater in the PBS group and in the female pups compared to the OMV treatment group (Fig 3D, Student's T-test **p** = 0.002 and 0.0095, respectively.) **(B, E, H)**: RT-qPCR of proinflammatory cytokines IL-1β, IL-6, and TNFα. **(C, F, I)**: RT-qPCR of anti-inflammatory cytokines IL-4, IL-10, and TGFβ. Total RNA was extracted from frozen whole brains and reverse transcribed to cDNA. Relative expression calculated by the $2^{\wedge-(\Delta\Delta Ct)}$ method with GAPDH as the reference gene. Group differences for the ELISAs on the males was not determined due to low sample size (n = 2). Only significant differences are shown. Data are presented with the median and 95% CI. Symbols: Circles = PBS, triangles = Pg; orange = females; blue = males.

https://doi.org/10.1371/journal.pone.0310482.g003

statistically different between the treatment groups (Fig 3A and 3G, p > 0.05 in both cases). We extended this analysis to include effects that may be apparent at the level of expression in the embryonic brain tissue. RT-qPCR analysis of these cytokines showed no significant difference between the PBS and Pg-OMV pups (Fig 3B, 3E and 3H). However, microglia are pleiotropic and can exist in multiple states when active. As Iba-1 is a general marker of microglia activation, it can not be used to differentiate microglia in the M1 state from those in the so-called M2 state where the production of anti-inflammatory cytokines may be observed [56,57]. Thus, we tested whether there was an anti-inflammatory immune response given that microglia can be in two broad functional categories when activated [43,56,58]. Analysis of IL-4, IL-10 and TGFβ typical of M2 activated microglia were not significantly different between the treatment groups (Fig 3C, 3F, 3I, p > 0.05 in all cases). Lastly, given these results

we tested whether the expression of NLRP3, MyD88 and NFκβ, that can be modified by exposure to Pg or it's OMV, were also modified in our pups. RT-qPCR analysis of MyD88 and NLRP3 transcripts (Fig 4) had similar downward trends with Pg-OMV treatment but were not significantly different compared to controls (Fig 4A, and 4B, p > 0.05 in both cases). Interestingly, NFkβ transcripts that are typically reported as being upregulated by Pg were significantly decreased in the Pg-OMV group (Fig 4C, Student's T-test p = 0.004). Full Western blots for Iba-1 can be found in the supporting information S2.

We were interested in identifying potential modifications in cytokine concentration and expression that may differ between female and male offspring as maternal inflammation may have sex specific effects. When parsed by sex, we observed that IL-6 and IL-1β concentrations were significantly lower in female pups from the Pg-OMV group compared to the female controls (Fig 3A, Mann-Whitney U test p = 0.04 and 3D, Student's T-test p = 0.0095) and though TNFα was lower in Pg-female pups, it was not statistically different in our analysis (Fig 3A, 3D. 3G). The effect of Pg-OMV on transcription was highly variable for IL-1β, TNFα, IL-4, IL-10 and TGFβ but generally trended upwards (Fig 3B–3I) for the female pups. Trends in the males were similar but were not significant and likely result from low sample sizes (Fig 3), though we could not assess difference in cytokine concentrations as the Pg male group had only 2 observations (Fig 3A, 3D, 3G).

Cortical neurons

Without a strong inflammatory phenotype, we tested the possibility that Pg-OMV treatment could nonetheless result in differences in the cortical neurons of the developing mouse brain. We examined the distribution of neuronal proteins Cux1, SatB2, and Ctip2 that are differentially expressed across the layers of the cortex in sagittal sections of embryonic mouse brains. The distribution and density of these proteins were modified by exposure to Pg-OMV compared to pups from the PBS group (Fig 5A and 5B). We saw significant decreases in Cux1 (Student's T-test p = 0.03) and SatB2 (Students T-test p = 0.0001) signal intensity but not Ctip2 (Student's T-test p = 0.064) although it also followed a similar downward trend in the Pg-OMV pup brains (Fig 5B). These findings suggests that cortical layering was drastically altered in Pg exposed animals.
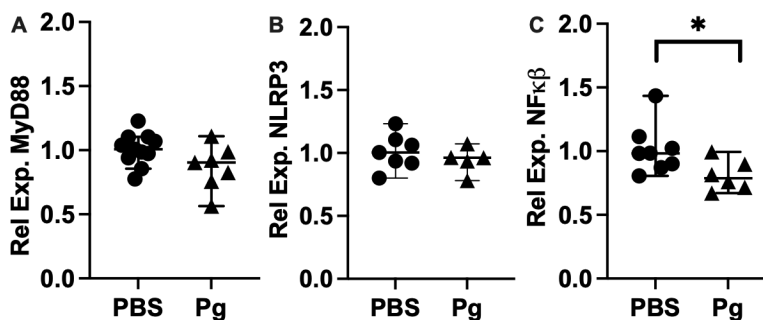
Fig 4. RT-qPCR evaluation of MYD88, NLRP3, and NFκβ in GA 18.5 pup brains. (A) MyD88 and **(B)** NLRP3 were not significantly different in pup brains from the control or treatment group. **(C)** NFkβ was significantly reduced in the pup brains (Student's T-test p = 0.004). Total RNA was extracted from frozen whole brains and reverse transcribed to cDNA. Relative expression calculated by the $2^{\wedge-(\Delta\Delta Ct)}$ method with GAPDH as the reference gene. Means across fore, mid, and hind brain sections are shown for each sample. Data are presented with the median value and 95% CI.

https://doi.org/10.1371/journal.pone.0310482.g004
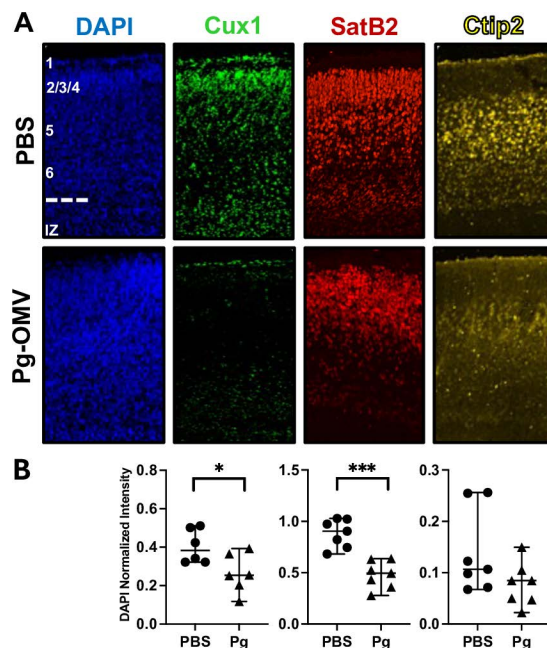
Fig 5. Modified intensity and location of cortical layer marker proteins following Pg-OMV exposure *in utero*. (A) Representative immunofluorescent images from sagittal sections of PFA fixed brains at GA 18.5 pup brains showing location of cortical layer markers Cux1, SatB2, and Ctip2. Approximate position of cortical layers 1–6 with the intraventricular zone (IZ) are shown in the PBS-DAPI image. **(B)** Quantification and comparison of cortical layer proteins stained with the marker antibodies. Intensities were averaged across three serial section per sample for statistical analysis. Cux1 (Student's T-test p = 0.03) and SatB2 (students T-test p = 0.0001) were significantly reduced in the Pg-OMV group. Data are presented with the median and 95% CI.

https://doi.org/10.1371/journal.pone.0310482.g005

Total Tau and p-TauThr231

We evaluated expression of total Tau and p-Tau Thr231 as potential markers of shifts in the embryonic Tau pool in response to maternal exposure to Pg-OMV. Western blot and probing with the anti-tau Tau5 antibody indicated a slight but not significant decrease in the mean total Tau concentration in brains from the Pg-OMV group compared to the PBS controls (Fig 6C, Student's t-test, p = 0.1761).

Probing with the anti-pTau Thr231 antibody demonstrated Tau was in a phosphorylated state concordant with other observations of Tau in the developing mouse brain (Fig 6A). Normalizing the p-Tau Thr231 against vinculin and total Tau showed that p-Tau Thr231 was significantly increased in the brains of embryos whose mothers were dosed with OMVs compared to the embryos of unexposed mothers (Fig 6D, Student's T-Test p = 0.0013, 6E Mann-Whitney U Test p = 0.0025).

Discussion

Animal models of Pg infection demonstrate modified pregnancy outcomes and can alter birth weight of offspring. Our experimental design did not recapitulate these observations as pup weights in the Pg-OMV group were not statistically different from PBS controls. Moreover, dam weights were also unchanged indicating that food and water intake were likely not different between the control and treatment groups. The mechanism behind reduced brain weight is not clear from our observations, although pup weight followed a
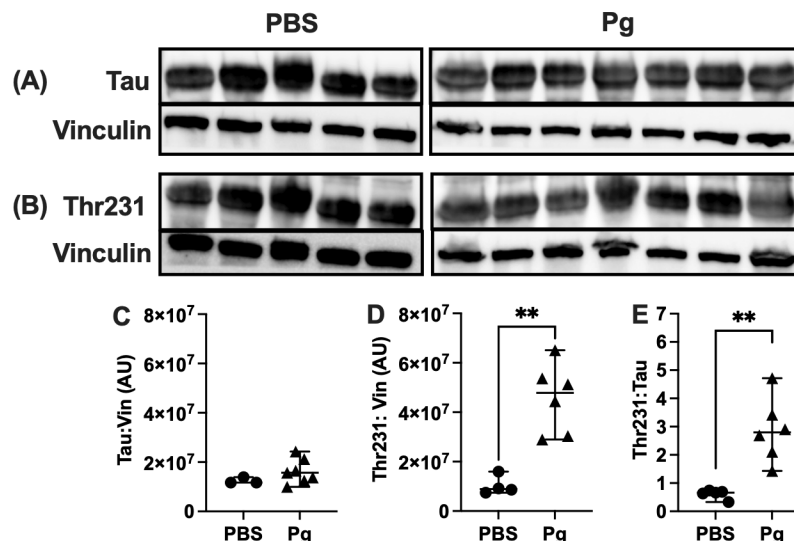
Fig 6. Differences in total Tau and p-Tau Thr231 following maternal Pg-OMV exposure. (A-B) Representative images of WB showing total Tau and p-Tau Thr231 Tau from E18.5 pup brains. **(C-D)** Quantification of western blots showing decrease in total Tau and increase in p-Tau Thr231 (Student's T-Test p = 0.0013). **(E)** Ratio of p-Tau to Total Tau was significantly increased in the Pg pups (Mann-Whitney U Test p = 0.0025). Data show mean +/- SEM.

https://doi.org/10.1371/journal.pone.0310482.g006

similar downward trend suggesting that the effect of Pg-OMV was systemic for the developing embryos. It could be possible that exposure to pathogens after initiation of pregnancy is different from a state where the pathogen is already present and interacting with host defense mechanisms. Likewise, the dosage of Pg-OMV we used may have not been sufficient to recapitulate the full effect of Pg on pregnancy outcomes, where more robust responses of the host and fetus may be required to lower birth weights. This would coincide with unchanged expression of Hif1a. Nevertheless, treatment with a low dosage of Pg-OMV during pregnancy impacted the development of the embryonic brain that could have implications after birth.

P. gingivalis and Pg-OMV iinduced neuroinflammation is suspected to be involved in cognitive decline in aging cohorts and have a significant impact on development *in utero*. Our hypothesis that maternal exposure to Pg-OMV would produce a pro-inflammatory response in the embryonic mouse brain was not supported. Cytokine concentrations and levels of mRNA transcripts in the pup brains tended to be lower in the Pg-OMV group. The lack of concordance with previous work was somewhat unexpected as most reports demonstrate an inflammatory response upon exposure to Pg or its OMV. Significant increases of Iba-1 the embryonic brain of Pg-OMV exposed dams could indicate sensing of bacterial-derived components, such as LPS, that can stimulate immune response, though this was not accompanied by a significant increase in cytokine production in our mice. Moreover, Pg has atypical LPS compared to organisms like *E. coli* LPS, that can bind to TLR-4, but can be recognized by alternative sensing pathways. We addressed this possibility by quantifying the expression of MyD88 and NLRP3 inflammasome mRNAs that are known to increase upon exposure to Pg or Pg-OMV. Our analysis found that concentrations of both were unaffected by OMV treatment in GA 18.5 pup brains. These relationships suggest direct interaction of Pg, OMV, or circulating virulence factors could be responsible for the observed phenotypes. However, microglia could be activated indirectly by Pg or Pg-OMV through maternal signals not quantified in this study. In either case there needs to be more work to clarify direct and indirect

fetal-pathogen interactions that modify development. We suspect several factors may be contributing to our observations. First, our results could originate from the delivery of Pg-OMV via tail vein injection which bypass sensing mechanisms such as dendritic cells of the gastrointestinal tract that would detect Pg and LPS being translocated from the oral cavity in saliva. Second, it is equally possible that Pg-OMV induced inflammation reported elsewhere may be an outcome in adult mice with long-term exposure to Pg or Pg-OMV but may not necessarily be an outcome for exposure after pregnancy has been established given the maternal immune system functions differently compared to the pre-pregnancy state. Thus, our observations may not be comparable to reports that use Pg infection or treatment with Pg or Pg-OMV at high doses over several weeks prior to inducing pregnancy. Importantly, the dosing scheme described here suggests there is a potential use of Pg-OMV as a proxy for bacteria to study effects on fetal tissues independent of systemic inflammation driven by common oral pathogens that become more prevalent during pregnancy. More work is needed to elucidate how the timing and dosage of pathogen exposure relative to the start of pregnancy modulates immune responses during gestation that could be associated with long-term consequences for offspring in human populations.

Several reports have quantified the impact of Pg and Pg-OMV on neurons as that cell type is affected by inflammation and is important in brain development. Our data indicate that Pg-OMV have a significant impact on neurons as their prevalence was modified in the cortical layers of the embryonic brain. Cux1, SatB2, and Ctip2 signals were lower overall and showed modified distribution in the Pg-OMV exposed brains compared to controls. The down regulation of SatB2 and Cux1 are particularly interesting as abnormal expression of both are associated with altered behavior in mice and are suspected to be a contributor to autism spectrum disorder-like symptoms in humans. Likewise, deficiencies in Cux1 expression have been linked to neurodevelopmental delays, while down regulation of Ctip2 is known to affect axonal growth and is involved in spiny neuron differentiation. The changes observed herein are aligned with previous studies, yet novel because these cortical layer aberrations were not accompanied by any indication of inflammation. Collectively, these data suggest that Pg, or perhaps Pg-OMV specially, affect the developing brain through a different mechanism. Parsing out the effects of Pg-OMV on cell proliferation and migration appears to be critical in deciphering how Pg mediates effects on the developing brain and should be addressed in future studies to better understand this important host-pathogen interaction.

The importance of Tau in the developing brain has not been fully described but our observations indicate maternal exposure to Pg-OMV can alter the amount of p-Tau Thr231 in mouse embryos. Tauopathies have multiple effects on the central nervous system including sustained inflammation through NFκβ signaling microglia that detects the pathogenic form of Tau in adult animal models. Our data would appear to support the notion that p-Tau Thr231 in the embryonic mouse brain is not pathogenic as an innate immune response, concordant with an inflammation-based hypothesis of neurodegenerative phenotypes, was not observed. Accordingly, we did not observe an increase in NFκβ that can encourage transcription of cytokines. We did not perform a comprehensive assessment of Tau phosphorylation sites, nor did we specifically address potential interactions between p-Tau and microglia. Nonetheless, the alteration of Thr231 abundance aids in explaining how changes in neuron migration and axon growth may result from exposure to Pg *in utero*; our observed changes in cortical layer markers could be the result of altered microtubule binding driven by altered p-Tau. Thus, much work remains to be done in elucidating the role of Pg and Pg-OMV on human neurodevelopment and cognitive trajectories from the early to elderly phases of life.

Methods

OMV isolation and characterization

Porphyromonas gingivalis strain ATCC 33277 was grown in anaerobic conditions (85% N_2, 10% CO_2, 5% H_2) using Tryptic Soy Broth (Difco cat# 211768) medium supplemented with 5.0 mg ml-1 hemin (ThermoFisher, cat# AAA1116503), 1.0 mg ml^{-1} menadione (MP Biomedicals, cat # 102259), and 0.5 g L^{-1} L-cysteine-HC (MP Biomedicals, cat # 101446). A cleared supernatant was produced by pelleting cells at 8000 rpm for 15 minutes followed by filtration of the supernatant through a 0.45 um membrane filter under low vacuum pressure. Using Sorvall 11.5 mL ultracentrifuge tubes and ultracrimp tube plugs, filtered supernatant was ultacentrifuged at 65,000 rpm for 1 hour at 4°C using a Sorvall WX Ultra 80 centrifuge. Immediately after centrifugation, supernatant was discarded and the pellet containing the OMV was resuspended in 500 uL of PBS [59]. The gingipain activity was quantified using the assay as described by Potempa and Nguyen using L-BAPNA (Millipore-Sigma cat# B3279) as the substrate and live Pg as positive control [60]. LPS was quantified by using the Pierce Chromogenic Endotoxin Quant Kit (ThermoFisher cat # A39552) as directed by the manufacturer. Assays were conducted in clear 96-well flat bottom plates and the absorbance read on a Synergy H1 multimode plate reader (BioTek). Transmission electron microscopy of OMV was performed by placing 10 ul of Pg OMV prep on a formvar coated copper grid for 1 minute. The liquid was then wicked off and UranyLess electron microscopy stain (Electron Microscopy Sciences, Hatfield, PA) was added directly to the grid for 15 seconds and then wicked off. Grids were dried for 10 minutes and imaged with a Hitachi H-7650 Transmission Electron Microscope transmission electron microscope. The total protein of the OMV were quantified using the Pierce BCA (ThermoFisher cat # 23227) assay with BSA as a standard. OMV preps were stored at -20°C for future use.

Animal breeding and care, dosing and tissue collection

2–3 month old C57/Bl6 mice (male and female) were purchased from Jackson Labs (Maine, USA). All animals were housed in the animal research core under 12 h light/dark cycle. Mice were bred and dams were checked for plugs 2 x /day. Once a plug was visible, the dam was removed and was marked as gestational day 0 (GA 0). Starting at E3, 50 µg Pg OMV were administered via tail vein injection every other day until GA 18.5. An equal volume of sterile PBS was used for the control group. Pregnant dams were anesthetized using isoflurane and pups were removed via C-sections (care and euthanization details in the following section). Pups were decapitated and whole brain and placenta were collected from each pup. Half of the pup brains were randomly chosen and fixed using 4% paraformaldehyde followed by 30% sucrose prior to being mounted in O.C.T. and frozen for Immunohistochemical and Immuno-fluorescent analysis. The remaining brains were snap frozen in a liquid N_2 at time of collection and used for protein, RNA, and DNA extraction. Fixed tissues were stored at 4°C and frozen tissues were stored at -80°C.

Humane endpoints were used to ensure the ethical treatment of animals and minimize suffering. Briefly, pregnant mice were dosed with OMVs every other day from GA 3 to GA17. Lab staff were trained in euthanasia techniques and tail vein injections but staff members from the Animal Resource Center at the Research Institute at Nationwide Children's Hospital administered the OMV via tail vein injection for this experiment. A total of 20 mice, 4 males and 16 females, were used for this with tissues coming from 8 dams. Pregnant mice were anesthetized at GA 18.5 using isoflurane for the duration of the C-section. Once all pups had been removed, euthanasia proceeded by transcardiac perfusion of a saline solution followed by ice cold 4% paraformaldehyde fixative with subsequent decapitation. Indications that mice

were in distress were monitored daily and included: decreased activity levels, lethargy, pallor, hunched posture, decreased grooming and rough fur, decreased fecal output, and a positive skin tent test for dehydration. Signs of dehydration would be treated with subcutaneous fluid replacement that if not resolved within 48 hours of the first observation would constitute meeting an endpoint for euthanization. Body weights for each mouse recorded every 48 hours and a decrease of 20% or greater mass over this time met endpoint criteria for euthanization. Any dams that met endpoint criteria prior to GA 18, or males that met criteria at any time, were euthanized by CO_2 asphyxiation and cervical dislocation on the day the animal met endpoint criteria. Fortunately, no animals met endpoint criteria prior to GA 18.5 and no deaths were recorded for the 18.5 day period of the experiment. Females that did not become pregnant and all males were euthanized by CO_2 asphyxiation and cervical dislocation at the conclusion of the experiment. All experimental procedures were approved by the IACUC under protocol AR21-00010.

Protein extraction, western blotting and ELISA

Protein from snap-frozen whole brains were extracted using RIPA Buffer (Cell Signaling Technology cat# 9806) with protease inhibitor cocktail (ThermoFisher cat# 87785). Concentration was determined prior to loading using the Pierce BCA Assay Kit with subsequent colorimetric detection using BioTek Synergy H1 microplate reader. Samples were denatured in Laemmli buffer at 95°C for 5 min. 50 μg total protein from each sample was loaded onto 10% Mini-PROTEAN® TGX™ Precast Protein Gels (Bio-Rad) and separated for 1 h at 150 V. Proteins were transferred onto nitrocellulose or PVDF membranes using Turbo transfer (Bio-Rad) for 7 min at 2.5 A. Membranes were incubated in Everyblot blocking buffer (Bio-Rad) for 1 h at RT. For Iba-1 probe, membranes were cut at 37 kDa marker and lower half was incubated with Iba1, top half was incubated with b-actin. For Tau and p-Tau Thr231, membranes were cut between 75 and 100 kDa marker. Top half was incubated with vinculin, bottom half was incubated Tau5 (ThermoFisher cat# AHB0042) or phospho-Tau Thr231 (Cell Signaling Technology cat # 71429). A control Tau protein (Acro BioSystems cat # TAU-H5147) with similar molecular mass as mouse Tau was run. All primary antibody incubations were overnight at 4°C. Membranes were washed in 1 X Tris-buffered saline with 0.1% Tween-20 (TBST) prior to a secondary incubation with either goat anti-mouse HRP or goat anti-rabbit HRP at a dilution of 1:3000 for 1 h at RT. Membranes were washed a second time with 1 X TBST prior to a 5 min incubation in ECL reagent (ThermoFisher, SuperSignal West Pico Plus ECL substrate kit, cat# 34577). Blots were imaged on a Bio-Rad Chemidoc. Densitometric analysis was performed in ImageLab Software (Bio-Rad). Target signals were normalized to a control protein on each blot of either Vinculin or β-actin. Aliquots of the RIPA extracted proteins (from above) were used to quantify the cytokines by ELISA for IL-1β (ThermoFisher IL-1 beta Mouse ELISA kit, cat # BMS6002), IL-6 (ThermoFisher IL-6 Mouse ELISA kit, cat # BMS603-2) and TNFα (ThermoFisher TNF alpha Mouse ELISA kit, cat # BMS607-3), from whole brains according to manufacturer's protocol. All samples were run in duplicate. The average from both wells was used for quantification. A full list of reagents and western blots can be found in the supporting information S4.

Nucleic acid extraction, PCR, and RT-qPCR

DNA and RNA was extracted for sexing embryonic mice and RT-qPCR analysis of cytokine mRNAs present in the pup brains. Nucleic acids were extracted from frozen whole brains using the Omega Bio-tek E.Z.N.A. kit according to manufacturer's protocol (cat# R6731-01). RNA and DNA concentrations were determined using Qubit Fluorometer (Applied Biosystems) prior to subsequent analysis. For sexing of pups we added 1 μL DNA to a reaction with

the Q5 Master Mix (New England Biolabs, cat # M0492S) and primer sets for amplification of the IL3 (For 5'- GGG ACT CCA AGC TTC AAT CA-3', Rev 5'- TGG AGG AAG AAA AGC AA-3') and Sry (For 5'-TGG GAC TGG TGA CAA TTG TC, Rev 5'-GAG TAC AGG TGT GCA GCT CT-3') genes [61]. PCR conditions were 95°C for 4.5 min followed by 33 cycles of 95°C for 35 s, 50°C for 1 min and 72°C for 1 min. PCR products were terminated with a final extension at 72°C for 5 min. Bands positive for both are labeled as male while samples only expressing IL3 are labeled as female.

cDNAs for RT-qPCR were made by adding 1000 ng RNA to a reaction using the High Capacity cDNA Reverse Transcription Kit (Applied Biosystems, cat# 4368814). 1 µL of cDNA was added per reaction with gene specific primer pair sets for GAPDH, IL-1β, IL-6, TNFα, IL-4, IL-10, TGFβ, MyD88, NFκB, NLRP3 for RT-qPCR (Integrated DNA Technologies, PrimeTime qPCR Primer Assay). All samples were run in triplicate on a QuantStudio6 Pro (Applied Biosystems) using the PowerUp SYBR Green Master Mix (ThermoFisher, cat # A25741). Cycling conditions are as follows: 95°C for 15s followed by 60 °C for 1 min for 40 cycles. Gene expression was measured using the QuantStudio6 Pro detection system and normalized to GAPDH. Ct values were averaged from each triplicate and used to calculate the relative expression by the $2^{-(\Delta\Delta Ct)}$ method with GAPDH as the reference gene.

Immunofluorescent staining

Fixed brains were embedded in OCT medium and 25 µm sagittal sections were collected by a cryostat. Sections were washed with PBS, blocked in PBS containing 0.1% tritonX-100, and 10% donkey serum and probed with and primary antibodies to Cux1 (Protein Tech 11733-1-AP; diluted 1:300), SatB2 (Abcam ab92446; diluted 1:100), and Ctip2 (Abcam ab-18465; diluted 1:500). Sections were then washed with PBS and incubated with Alexa Fluor® secondary antibodies (ThermoFisher Scientific) and DAPI followed by mounting with Prolong Diamond Antifade (ThermoFisher Scientific). Images were acquired with an ImageXpress Micro Confocal High Content Imaging System (IXMC; Molecular Devices) and analyzed using MetaXpress software (Molecular Devices).

Data analysis

We used the analysis routines in GraphPad PRISM v. 10.0 to perform statistical analysis and plotting of data points. Outlier data points were identified by the ROUT method with Q = 1% and removed from analysis. Data were tested for normality with the Kolmogorov-Smirnov test. Group differences for data with normal distributions were tested with the two-tailed, unpaired Student's-test, otherwise statistical differences were determined with the Mann Whitney-U test. Data are presented with the median and 95% Confidence Interval (CI).

Supporting Information

S1 File. OMV TEM, gingipain activity and LPS quantification plots.
(PDF)

S2 File. IBA-1, Tau and p-TauThr231 western blots.
(PDF)

S3 Data. Data for figures.
(XLSX)

S4 File. Reagent list.
(XLSX)

Acknowledgments

Author contributions

Conceptualization: Lauren Mashburn-Warren, Lexie C. Blalock, Christian Lauber.

Formal analysis: Adrienne J. Bradley, Lauren Mashburn-Warren, Lexie C. Blalock, Christian Lauber.

Investigation: Adrienne J. Bradley, Lauren Mashburn-Warren, Lexie C. Blalock, Francesca Scarpetti.

Methodology: Adrienne J. Bradley, Lauren Mashburn-Warren, Lexie C. Blalock.

Project administration: Christian Lauber.

Resources: Christian Lauber.

Supervision: Christian Lauber.

Visualization: Adrienne J. Bradley, Lauren Mashburn-Warren, Christian Lauber.

Writing – original draft: Adrienne J. Bradley, Christian Lauber.

Writing – review & editing: Adrienne J. Bradley, Lauren Mashburn-Warren, Lexie C. Blalock, Francesca Scarpetti, Christian Lauber.

References

1. Carrillo-de-Albornoz A, Figuero E, Herrera D, Bascones-Martínez A. Gingival changes during pregnancy: II. influence of hormonal variations on the subgingival biofilm. J Clin Periodontol. 2010;37(3):230–40. https://doi.org/10.1111/j.1600-051X.2009.01514.x PMID: 20088983

2. Fujiwara N, Tsuruda K, Iwamoto Y, Kato F, Odaki T, Yamane N, et al. Significant increase of oral bacteria in the early pregnancy period in Japanese women. J Investig Clin Dent. 2017;8(1):e2189. https://doi.org/10.1111/jicd.12189 PMID: 26345599

3. Lin W, Jiang W, Hu X, Gao L, Ai D, Pan H, et al. Ecological shifts of supragingival microbiota in association with pregnancy. Front Cell Infect Microbiol. 2018;8:24. https://doi.org/10.3389/fcimb.2018.00024 PMID: 29497601

4. Paropkari AD, Leblebicioglu B, Christian LM, Kumar PS. Smoking, pregnancy and the subgingival microbiome. Scientific Reports. 2016;6(1):30388.

5. Jang H, Patoine A, Wu T, Castillo D, Xiao J. Oral microflora and pregnancy: a systematic review and meta-analysis. Scientific Reports. 2021;11(1):16870.

6. Powell AM, Khan FZA, Ravel J, Elovitz MA. Untangling associations of microbiomes of pregnancy and preterm birth. Clin Perinatol. 2024;51(2):425–39. https://doi.org/10.1016/j.clp.2024.02.009 PMID: 38705650

7. Wen P, Li H, Xu X, Zhang F, Zhao D, Yu R, et al. A prospective study on maternal periodontal diseases and neonatal adverse outcomes. Acta Odontol Scand. 2024;83:348–55. https://doi.org/10.2340/aos.v83.40836 PMID: 38860278

8. Kassebaum NJ, Bernabé E, Dahiya M, Bhandari B, Murray CJL, Marcenes W. Global burden of severe periodontitis in 1990-2010: a systematic review and meta-regression. J Dent Res. 2014;93(11):1045–53. https://doi.org/10.1177/0022034514552491 PMID: 25261053

9. Lieff S, Boggess KA, Murtha AP, Jared H, Madianos PN, Moss K, et al. The oral conditions and pregnancy study: periodontal status of a cohort of pregnant women. J Periodontol. 2004;75(1):116–26. https://doi.org/10.1902/jop.2004.75.1.116 PMID: 15025223

10. Kornman KS, Loesche WJ. The subgingival microbial flora during pregnancy. J Periodontal Res. 1980;15(2):111–22. https://doi.org/10.1111/j.1600-0765.1980.tb00265.x PMID: 6103927

11. Reyes L, Phillips P, Wolfe B, Golos TG, Walkenhorst M, Progulske-Fox A, et al. Porphyromonas gingivalis and adverse pregnancy outcome. J Oral Microbiol. 2017;10(1):1374153. https://doi.org/10.1080/20002297.2017.1374153 PMID: 29291034

12. Silva de Araujo Figueiredo C, Gonçalves Carvalho Rosalem C, Costa Cantanhede AL, Abreu Fonseca Thomaz ÉB, Fontoura Nogueira da Cruz MC. Systemic alterations and their oral manifestations in pregnant women. J Obstet Gynaecol Res. 2017;43(1):16–22. https://doi.org/10.1111/jog.13150 PMID: 28074549

13. Chaparro A, Blanlot C, Ramírez V, Sanz A, Quintero A, Inostroza C, et al. Porphyromonas gingivalis, Treponema denticola and toll-like receptor 2 are associated with hypertensive disorders in placental tissue: a case-control study. J Periodontal Res. 2013;48(6):802–9. https://doi.org/10.1111/jre.12074 PMID: 23711357

14. Ercan E, Eratalay K, Deren O, Gur D, Ozyuncu O, Altun B, et al. Evaluation of periodontal pathogens in amniotic fluid and the role of periodontal disease in pre-term birth and low birth weight. Acta Odontol Scand. 2013;71(3–4):553–9. https://doi.org/10.3109/00016357.2012.697576 PMID: 23638858

15. Gonzales-Marin C, Spratt DA, Millar MR, Simmonds M, Kempley ST, Allaker RP. Levels of periodontal pathogens in neonatal gastric aspirates and possible maternal sites of origin. Mol Oral Microbiol. 2011;26(5):277–90. https://doi.org/10.1111/j.2041-1014.2011.00616.x PMID: 21896155

16. Katz J, Chegini N, Shiverick KT, Lamont RJ. Localization of P. gingivalis in preterm delivery placenta. J Dent Res. 2009;88(6):575–8. https://doi.org/10.1177/0022034509338032 PMID: 19587165

17. León R, Silva N, Ovalle A, Chaparro A, Ahumada A, Gajardo M, et al. Detection of Porphyromonas gingivalis in the amniotic fluid in pregnant women with a diagnosis of threatened premature labor. J Periodontol. 2007;78(7):1249–55. https://doi.org/10.1902/jop.2007.060368 PMID: 17608580

18. Swati P, Ambika Devi K, Thomas B, Vahab SA, Kapaettu S, Kushtagi P. Simultaneous detection of periodontal pathogens in subgingival plaque and placenta of women with hypertension in pregnancy. Arch Gynecol Obstet. 2012;285(3):613–9. https://doi.org/10.1007/s00404-011-2012-9 PMID: 21830010

19. Ishida E, Furusho H, Renn T-Y, Shiba F, Chang H-M, Oue H, et al. Mouse maternal odontogenic infection with Porphyromonas gingivalis induces cognitive decline in offspring. Frontiers in Pediatrics. 2023;11.

20. Lara B, Loureiro I, Gliosca L, Castagnola L, Merech F, Gallino L, et al. Porphyromonas gingivalis outer membrane vesicles shape trophoblast cell metabolism impairing functions associated to adverse pregnancy outcome. J Cell Physiol. 2023;238(11):2679–91. https://doi.org/10.1002/jcp.31138 PMID: 37842869

21. Ao M, Miyauchi M, Furusho H, Inubushi T, Kitagawa M, Nagasaki A, et al. dental infection of porphyromonas gingivalis induces preterm birth in mice. PLoS One. 2015;10(8):e0137249. https://doi.org/10.1371/journal.pone.0137249 PMID: 26322971

22. Konishi H, Urabe S, Miyoshi H, Teraoka Y, Maki T, Furusho H, et al. Fetal membrane inflammation induces preterm birth Via Toll-Like receptor 2 in mice with chronic gingivitis. Reprod Sci. 2019;26(7):869–78. https://doi.org/10.1177/1933719118792097 PMID: 30223727

23. Konishi H, Urabe S, Teraoka Y, Morishita Y, Koh I, Sugimoto J, et al. Porphyromonas gingivalis, a cause of preterm birth in mice, induces an inflammatory response in human amnion mesenchymal cells but not epithelial cells. Placenta. 2020;99:21–6. https://doi.org/10.1016/j.placenta.2020.07.016 PMID: 32738645

24. Lin D, Smith MA, Champagne C, Elter J, Beck J, Offenbacher S. Porphyromonas gingivalis infection during pregnancy increases maternal tumor necrosis factor alpha, suppresses maternal interleukin-10, and enhances fetal growth restriction and resorption in mice. Infect Immun. 2003;71(9):5156–62. https://doi.org/10.1128/IAI.71.9.5156-5162.2003 PMID: 12933859

25. Yoshida S, Hatasa M, Ohsugi Y, Tsuchiya Y, Liu A, Niimi H, et al. Porphyromonas gingivalis administration induces gestational obesity, alters gene expression in the liver and brown adipose tissue in pregnant mice, and causes underweight in fetuses. Front Cell Infect Microbiol. 2022;11745117. https://doi.org/10.3389/fcimb.2021.745117 PMID: 35096633

26. Choi J-W, Kim S-C, Hong S-H, Lee H-J. Secretable small RNAs via outer membrane vesicles in periodontal pathogens. J Dent Res. 2017;96(4):458–66. https://doi.org/10.1177/0022034516685071 PMID: 28068479

27. Gui MJ, Dashper SG, Slakeski N, Chen Y-Y, Reynolds EC. Spheres of influence: Porphyromonas gingivalis outer membrane vesicles. Mol Oral Microbiol. 2016;31(5):365–78. https://doi.org/10.1111/omi.12134 PMID: 26466922

28. Ho M-H, Chen C-H, Goodwin JS, Wang B-Y, Xie H. Functional advantages of porphyromonas gingivalis vesicles. PLoS One. 2015;10(4):e0123448. https://doi.org/10.1371/journal.pone.0123448 PMID: 25897780

29. Okamura H, Hirota K, Yoshida K, Weng Y, He Y, Shiotsu N, et al. Outer membrane vesicles of Porphyromonas gingivalis: novel communication tool and strategy. Jpn Dent Sci Rev. 2021;57138–46. https://doi.org/10.1016/j.jdsr.2021.07.003 PMID: 34484474

30. Veith PD, Chen Y-Y, Gorasia DG, Chen D, Glew MD, O'Brien-Simpson NM, et al. Porphyromonas gingivalis outer membrane vesicles exclusively contain outer membrane and periplasmic proteins and carry a cargo enriched with virulence factors. J Proteome Res. 2014;13(5):2420–32. https://doi.org/10.1021/pr401227e PMID: 24620993

31. Zhang J, Yu C, Zhang X, Chen H, Dong J, Lu W, et al. Porphyromonas gingivalis lipopolysaccharide induces cognitive dysfunction, mediated by neuronal inflammation via activation of the TLR4 signaling pathway in C57BL/6 mice. J Neuroinflammation. 2018;15(1):37. https://doi.org/10.1186/s12974-017-1052-x PMID: 29426327

32. Nara PL, Sindelar D, Penn MS, Potempa J, Griffin WST. Porphyromonas gingivalis outer membrane vesicles as the major driver of and explanation for neuropathogenesis, the cholinergic hypothesis, iron dyshomeostasis, and salivary lactoferrin in Alzheimer's disease. J Alzheimers Dis. 2021;82(4):1417–50. https://doi.org/10.3233/JAD-210448 PMID: 34275903

33. Gong T, Chen Q, Mao H, Zhang Y, Ren H, Xu M. Outer membrane vesicles of Porphyromonas gingivalis trigger NLRP3 inflammasome and induce neuroinflammation, tau phosphorylation, and memory dysfunction in mice. Front Cell Infect Microbiol. 2022;12:925435.

34. Lan C, Chen S, Jiang S, Lei H, Cai Z, Huang X. Different expression patterns of inflammatory cytokines induced by lipopolysaccharides from Escherichia coli or Porphyromonas gingivalis in human dental pulp stem cells. BMC Oral Health. 2022;22(1):121. https://doi.org/10.1186/s12903-022-02161-x PMID: 35413908

35. Qiu C, Yuan Z, He Z, Chen H, Liao Y, Li S, et al. Lipopolysaccharide preparation derived from Porphyromonas gingivalis induces a weaker immuno-inflammatory response in BV-2 microglial cells than escherichia coli by differentially activating TLR2/4-Mediated NF-κB/STAT3 signaling pathways. Front Cell Infect Microbiol. 2021;11:606986. https://doi.org/10.3389/fcimb.2021.606986 PMID: 33816329

36. Bodet C, Chandad F, Grenier D. Modulation of cytokine production by Porphyromonas gingivalis in a macrophage and epithelial cell co-culture model. Microbes Infect. 2005;7(3):448–56. https://doi.org/10.1016/j.micinf.2004.11.021 PMID: 15811635

37. Castillo Y, Castellanos JE, Lafaurie GI, Castillo DM. Porphyromonas gingivalis outer membrane vesicles modulate cytokine and chemokine production by gingipain-dependent mechanisms in human macrophages. Arch Oral Biol. 2022;140:105453. https://doi.org/10.1016/j.archoralbio.2022.105453 PMID: 35580388

38. Charoensaensuk V, Chen Y-C, Lin Y-H, Ou K-L, Yang L-Y, Lu D-Y. Porphyromonas gingivalis induces proinflammatory cytokine expression leading to apoptotic death through the oxidative stress/NF-κb pathway in brain endothelial cells. Cells. 2021;10(11):3033. https://doi.org/10.3390/cells10113033 PMID: 34831265

39. Palm E, Khalaf H, Bengtsson T. Porphyromonas gingivalis downregulates the immune response of fibroblasts. BMC Microbiol. 2013;13:155. https://doi.org/10.1186/1471-2180-13-155 PMID: 23841502

40. Yang K, Xu S, Zhao H, Liu L, Lv X, Hu F, et al. Hypoxia and Porphyromonas gingivalis-lipopolysaccharide synergistically induce NLRP3 inflammasome activation in human gingival fibroblasts. Int Immunopharmacol. 2021;94:107456. https://doi.org/10.1016/j.intimp.2021.107456 PMID: 33588175

41. Offenbacher S, Katz V, Fertik G, Collins J, Boyd D, Maynor G, et al. Periodontal infection as a possible risk factor for preterm low birth weight. J Periodontol. 1996;67(10 Suppl):1103–13. https://doi.org/10.1902/jop.1996.67.10s.1103 PMID: 8910829

42. Ostrem BEL, Domínguez-Iturza N, Stogsdill JA, Faits T, Kim K, Levin JZ, et al. Fetal brain response to maternal inflammation requires microglia. Development. 2024;151(10):dev202252. https://doi.org/10.1242/dev.202252 PMID: 38775708

43. Zhang B, Wei Y-Z, Wang G-Q, Li D-D, Shi J-S, Zhang F. Targeting MAPK Pathways by naringenin modulates microglia M1/M2 polarization in lipopolysaccharide-stimulated cultures. Front Cell Neurosci. 2019;12:531. https://doi.org/10.3389/fncel.2018.00531 PMID: 30687017

44. Frank-Cannon TC, Alto LT, McAlpine FE, Tansey MG. Does neuroinflammation fan the flame in neurodegenerative diseases?. Mol Neurodegener. 2009;4:47. https://doi.org/10.1186/1750-1326-4-47 PMID: 19917131

45. Gao Y, Tan L, Yu J-T, Tan L. Tau in Alzheimer's disease: mechanisms and therapeutic strategies. Curr Alzheimer Res. 2018;15(3):283–300. https://doi.org/10.2174/1567205014666170417111859 PMID: 28413986

46. Morris SL, Brady ST. Tau phosphorylation and PAD exposure in regulation of axonal growth. Front Cell Dev Biol. 2023;10:1023418. https://doi.org/10.3389/fcell.2022.1023418 PMID: 36742197

47. Seubert P, Mawal-Dewan M, Barbour R, Jakes R, Goedert M, Johnson GV, et al. Detection of phosphorylated Ser262 in fetal tau, adult tau, and paired helical filament tau. J Biol Chem. 1995;270(32):18917–22. https://doi.org/10.1074/jbc.270.32.18917 PMID: 7642549

48. Brion JP, Smith C, Couck AM, Gallo JM, Anderton BH. Developmental changes in tau phosphorylation: fetal tau is transiently phosphorylated in a manner similar to paired helical filament-tau characteristic of Alzheimer's disease. J Neurochem. 1993;61(6):2071–80. https://doi.org/10.1111/j.1471-4159.1993.tb07444.x PMID: 8245963

49. Tang Z, Liang D, Cheng M, Su X, Liu R, Zhang Y, et al. Effects of porphyromonas gingivalis and its underlying mechanisms on alzheimer-like Tau Hyperphosphorylation in sprague-dawley rats. J Mol Neurosci. 2021;71(1):89–100. https://doi.org/10.1007/s12031-020-01629-1 PMID: 32557144

50. Yu Y, Run X, Liang Z, Li Y, Liu F, Liu Y. Developmental regulation of tau phosphorylation, tau kinases, and tau phosphatases. J Neurochem. 2009;108(6):1480–94.

51. Arendt T, Stieler JT, Holzer M. Tau and tauopathies. Brain Res Bull. 2016;126(Pt 3):238–92. https://doi.org/10.1016/j.brainresbull.2016.08.018 PMID: 27615390

52. Wang C, Fan L, Khawaja R, Liu B, Zhan L, Kodama L, et al. Microglial NF-κB drives tau spreading and toxicity in a mouse model of tauopathy. Nature Communications. 2022;13(1):1969. https://doi.org/10.1038/ncomms1969

53. Perea JR, Ávila J, Bolós M. Dephosphorylated rather than hyperphosphorylated Tau triggers a pro-inflammatory profile in microglia through the p38 MAPK pathway. Exp Neurol. 2018;310:14–21. https://doi.org/10.1016/j.expneurol.2018.08.007 PMID: 30138606

54. Hefti M, Kim S, Bell A, Betters R, Fiock K, Iida M. Tau phosphorylation and aggregation in the developing human brain. J Neuropathol Exp Neurol. 2019;78(10):930–8.

55. Sapir T, Frotscher M, Levy T, Mandelkow E-M, Reiner O. Tau's role in the developing brain: implications for intellectual disability. Hum Mol Genet. 2012;21(8):1681–92. https://doi.org/10.1093/hmg/ddr603 PMID: 22194194

56. Smith JA, Das A, Ray SK, Banik NL. Role of pro-inflammatory cytokines released from microglia in neurodegenerative diseases. Brain Res Bull. 2012;87(1):10–20. https://doi.org/10.1016/j.brainresbull.2011.10.004 PMID: 22024597

57. Walker DG, Lue L-F. Immune phenotypes of microglia in human neurodegenerative disease: challenges to detecting microglial polarization in human brains. Alzheimers Res Ther. 2015;7(1):56. https://doi.org/10.1186/s13195-015-0139-9 PMID: 26286145

58. Mishra A, Bandopadhyay R, Singh PK, Mishra PS, Sharma N, Khurana N. Neuroinflammation in neurological disorders: pharmacotherapeutic targets from bench to bedside. Metab Brain Dis. 2021;36(7):1591–626. https://doi.org/10.1007/s11011-021-00806-4 PMID: 34387831

59. Mashburn LM, Whiteley M. Membrane vesicles traffic signals and facilitate group activities in a prokaryote. Nature. 2005;437(7057):422–5. https://doi.org/10.1038/nature03925 PMID: 16163359

60. Potempa J, Nguyen K-A. Purification and characterization of gingipains. Curr Protoc Protein Sci. 2007;Chapter 21:21.20.1–27. https://doi.org/10.1002/0471140864.ps2120s49 PMID: 18429320

61. Lambert JF, Benoit BO, Colvin GA, Carlson J, Delville Y, Quesenberry PJ. Quick sex determination of mouse fetuses. J Neurosci Methods. 2000;95(2):127–32. https://doi.org/10.1016/s0165-0270(99)00157-0 PMID: 10752483